

Original Article

Detection of Adulterants in the Essential Oil by *Curcuma aeruginosa* Roxb. FTIR Spectroscopy and Multivariate Analysis

Bekti Nugraheni^{1*}, Ratna Asmah Susidarti², Purwanto³, and Abdul Rohman²

¹Sekolah Tinggi Ilmu Farmasi (STIFAR) Yayasan Pharmasi Semarang, Semarang, Central Java, Indonesia

²Department of Pharmaceutical Chemistry, Faculty of Pharmacy, Universitas Gadjah Mada, Yogyakarta, Indonesia

³Department of Pharmaceutical Biology, Faculty of Pharmacy, Universitas Gadjah Mada, Yogyakarta, Indonesia

*Corresponding author: Bekti Nugraheni | Email: bektinugraheni@stifar.ac.id

Received: 27 October 2025; Revised: 06 March 2026; Accepted: 10 April 2026; Published: 13 June 2026

Abstract: Authentication of *Curcuma aeruginosa* Roxb. essential oils (EOs-CA) is critical to prevent adulteration and to ensure the quality and safety of derived products. This study aimed to evaluate the effectiveness of Fourier Transform Infrared (FTIR) spectroscopy in combination with chemometric methods for the authentication of EOs-CA, particularly in the presence of adulterants such as Virgin Coconut Oil (VCO). VCO was selected as an adulterant model due to its spectral similarity with EOs-CA. Discriminant Analysis (DA) and multivariate calibration techniques—Partial Least Squares (PLS) and Principal Component Regression (PCR)—were employed for the classification and quantification of adulterated EOs-CA samples, including those mixed with *Curcuma xanthorrhiza* essential oil (EOs-CX). A total of 26 samples were prepared, comprising binary mixtures of EOs-CA/EOs-CX and ternary mixtures of EOs-CA/EOs-CX/VCO, with adulterant concentration levels ranging from 0% to 100%. FTIR spectral data were collected in the wavenumber range of 4000–650 cm⁻¹ using an Agilent Cary 630 FTIR-ATR spectrophotometer (USA). Chemometric analyses were conducted using DA, PLS, and PCR methods through TQ Analyst software version 9 (Thermo Fisher Scientific, Inc.). The DA method successfully classified authentic and adulterated samples with accuracy rates of 99.99% and 99.96% for the binary and ternary systems, respectively. Quantitative determination of EOs-CA in binary mixtures with EOs-CX was achieved using the second derivative of FTIR spectra in the 1770–728 cm⁻¹ region, yielding coefficients of determination (R²) of 0.9992 and 0.9994 for the calibration and validation models, respectively. The Root Mean Square Error of Calibration (RMSEC) and Prediction (RMSEP) were 1.19% and 1.16%, respectively. These findings demonstrate that FTIR spectroscopy combined with chemometric techniques provides a reliable and accurate method for detecting adulteration and authenticating EOs-CA against potential adulterants such as EOs-CX and VCO.

Keywords: chemometrics, *curcuma aeruginosa*, *curcuma xanthorrhiza*, virgin coconut oil, ftir spectroscopy

1. INTRODUCTION

Indonesia possesses the second-highest biodiversity in the world, encompassing a wide range of ecosystems, genetic resources, and plant species diversity [1-2]. The therapeutic and health benefits of native Indonesian plants have long been recognized and utilized, particularly species belonging to the *Zingiberaceae* family. Among these are *Curcuma xanthorrhiza*, *Curcuma longa*, *Curcuma zedoaria*, *Curcuma hyneana*, and *Curcuma aeruginosa* [3]. The rhizome of *Curcuma aeruginosa* (*C. aeruginosa*) is the most widely used part for medicinal purposes [4-5]. It is rich in lipophilic essential oils, which are commonly extracted through hydrodistillation or steam distillation from fresh rhizomes (6-7). The quality of essential oils of *C. aeruginosa* (EOs-CA), particularly when used as raw material in traditional medicine, is largely determined by their chemical composition and corresponding biological activities. EOs-CA is predominantly composed of oxygenated sesquiterpenes (42.85%), hydrocarbon sesquiterpenes (30.80%), oxygenated monoterpenes (10.92%), and hydrocarbon monoterpenes (10.82%) [8]. Among the bioactive compounds, germacrone (5.3%) and curzerenone (59.60%) have been identified as the major constituents [9].

Numerous studies have demonstrated that EOs-CA possesses strong antibacterial [10-11] and antioxidant activities [8, 10]. Antioxidant activity evaluated in vitro using 2,2-diphenyl-1-picrylhydrazyl (DPPH) and nitric oxide (NO) radical scavenging assays yielded effective concentration (EC_{50}) values of 30 and 28 $\mu\text{g/mL}$, respectively [10]. In addition, hydroxyl (OH) radical scavenging activity recorded an EC_{50} of 244.48 $\mu\text{g/mL}$, further supporting the strong antioxidant potential of EOs-CA. Antibacterial assays have demonstrated EOs-CA's inhibitory effects against *Staphylococcus aureus*, *Streptococcus mutans*, and *Escherichia coli*. Microdilution assays in tryptic soy broth (TSB) revealed that *S. aureus* had the lowest minimum inhibitory concentration (MIC) and minimum bactericidal concentration (MBC) values of 7.81 and 250 $\mu\text{g/mL}$, respectively [8]. In another study using Mueller-Hinton Broth (MHB), MIC values of 125 $\mu\text{g/mL}$ were recorded for both *S. aureus* and *Bacillus cereus*, suggesting that EOs-CA is generally more effective against Gram-positive bacteria than Gram-negative strains such as *Pseudomonas aeruginosa* and *E. coli*. Furthermore, tests comparing EOs-CA from dry and fresh rhizomes demonstrated strong antibacterial activity against *Bacillus subtilis*, with MIC values of 6.25 and 12.5 $\mu\text{g/mL}$, respectively [12]. These findings confirm that EOs-CA exhibits strong MIC values [13-14]. Given its potent antioxidant and antibacterial properties, EOs-CA holds significant commercial value in the essential oil market. However, this high value also renders it vulnerable to adulteration, often through blending with cheaper oils to increase profit margins. Therefore, the development of rapid and reliable analytical methods is essential for detecting adulteration and ensuring the authenticity and quality of EOs-CA in both pharmaceutical and commercial applications.

Various analytical techniques have been employed to detect adulteration in essential oil products, including chromatography-based methods such as High-Performance Liquid Chromatography (HPLC), Thin-Layer Chromatography (TLC), and Gas Chromatography (GC), as well as spectroscopic techniques such as Ultraviolet-Visible (UV-Vis) spectroscopy, Nuclear Magnetic Resonance (NMR), Mass Spectrometry (MS), Near-Infrared (NIR) spectroscopy, and Fourier-Transform Infrared (FTIR) spectroscopy [15-16]. Among these, FTIR spectroscopy combined with multivariate calibration has been widely utilized in recent studies for the authentication and quality control of essential oil products [17]. Notable applications include the authentication of *Nigella sativa* oil from corn and soybean oil adulterants [18], detection of *Curcuma mangga* adulteration with candlenut oil [18], turmeric EOs authenticity [19], identification and quantification of counterfeit lavender oil adulterated with citronella oil [20], and differentiation of *Mentha spicata* essential oil and l-menthol in *Mentha piperita* [21]. In this study, the adulterants used were EOs-CX and VCO. Although both materials have relatively high economic value, they are still commonly employed as adulterants due to differences in market price and availability. The EOs-CA has a low yield and limited production, resulting in a higher and more fluctuating market price. In contrast, VCO is widely produced in Indonesia and readily available in large volumes, making it suitable as a diluent. Likewise, EOs-CX has an aroma profile and chemical fingerprint similar to that of EOs-CA and is generally easier to obtain through large-scale production. Therefore, this study employed FTIR spectroscopy combined with multivariate analysis techniques to authenticate EOs-CA against adulteration by EOs-CX and VCO in both binary and ternary mixtures.

2. MATERIALS AND METHODS

2.1. Materials

Fresh rhizomes of *Curcuma aeruginosa* (CA) and *Curcuma xanthorrhiza* (CX) were used in this study. Both plant samples were taxonomically identified at the Department of Pharmaceutical Biology, Faculty of Pharmacy, Universitas Gadjah Mada, Yogyakarta, Indonesia. Virgin Coconut Oil (VCO) was procured from a local store in Semarang, Central Java. The chemical reagent used for drying the extracted oils was anhydrous sodium sulfate (Smart-lab).

2.2. Methods

2.2.1. Sample collection and preparation

Fresh rhizomes of *Curcuma aeruginosa* (CA) and *Curcuma xanthorrhiza* (CX) were sliced into pieces approximately 1–2 cm thick. The sliced rhizomes were subjected to steam distillation over

medium heat for eight hours. Anhydrous sodium sulfate was added to the resulting distillate to remove residual moisture, followed by centrifugation at 2500 rpm for 5 minutes using a Thermo Scientific centrifuge. The yield of the essential oil was calculated as a percentage of the total distillate obtained. Virgin Coconut Oil (VCO) was used as an adulterant.

2.2.2. Preparation of Oil Samples

Calibration samples of EOs-CA were prepared in both binary and ternary mixtures with EOs-CX and VCO. The adulterant concentrations were varied from 0% to 100% (v/v), as detailed in Tables 1 and 2.

Table 1. The binary mixtures of EOs-CA and EOs-CX used for FTIR Analysis

| Samples | EOs-CA (%) | EOs-CX (%) | Samples | EOs-CA (%) | EOs-CX (%) |
|---------|------------|------------|---------|------------|------------|
| 1 | 100 | 0 | 14 | 48 | 52 |
| 2 | 96 | 4 | 15 | 44 | 56 |
| 3 | 92 | 8 | 16 | 40 | 60 |
| 4 | 88 | 12 | 17 | 36 | 64 |
| 5 | 84 | 16 | 18 | 32 | 68 |
| 6 | 80 | 20 | 19 | 28 | 72 |
| 7 | 76 | 24 | 20 | 24 | 76 |
| 8 | 72 | 28 | 21 | 20 | 80 |
| 9 | 68 | 32 | 22 | 16 | 84 |
| 10 | 64 | 36 | 23 | 12 | 88 |
| 11 | 60 | 40 | 24 | 8 | 92 |
| 12 | 56 | 44 | 25 | 4 | 96 |
| 13 | 52 | 48 | 26 | 0 | 100 |

Table 2. The ternary mixtures of EOs-CA and EOs-CX/VCO used for FTIR Analysis

| Samples | EOs-CA (%) | VCO (%) | EOs-CX (%) | Samples | EOs-CA (%) | VCO (%) | EOs-CX (%) |
|---------|------------|---------|------------|---------|------------|---------|------------|
| 1 | 100 | 0 | 0 | 14 | 46 | 10 | 44 |
| 2 | 0 | 100 | 0 | 15 | 50 | 33 | 17 |
| 3 | 0 | 0 | 100 | 16 | 49 | 8 | 43 |
| 4 | 42 | 23 | 35 | 17 | 27 | 45 | 28 |
| 5 | 38 | 0 | 62 | 18 | 26 | 15 | 59 |
| 6 | 40 | 14 | 46 | 19 | 49 | 37 | 14 |
| 7 | 15 | 41 | 44 | 20 | 19 | 34 | 23 |
| 8 | 58 | 11 | 31 | 21 | 48 | 24 | 28 |
| 9 | 22 | 34 | 44 | 22 | 46 | 14 | 40 |
| 10 | 31 | 41 | 29 | 23 | 20 | 15 | 65 |
| 11 | 23 | 49 | 38 | 24 | 11 | 38 | 51 |
| 12 | 6 | 36 | 58 | 25 | 17 | 40 | 53 |
| 13 | 69 | 2 | 29 | 26 | 46 | 49 | 5 |

2.2.3. FTIR Spectroscopic Analysis

FTIR spectra were recorded using a Cary 630 FTIR spectrophotometer (Agilent Technologies, USA), equipped with an Attenuated Total Reflectance (ATR) accessory. Spectra were collected in absorbance mode over the range of 4000–650 cm^{-1} at a resolution of 8 cm^{-1} , with 32 scans per sample. Data acquisition and processing were performed using MicroLab Expert software. All spectral analyses were conducted at room temperature.

2.2.4. Data Analyses

Chemometric analyses were performed using Discriminant Analysis (DA) for classification and Partial Least Squares (PLS) and Principal Component Regression (PCR) for multivariate calibration. The analysis was carried out using TQ Analyst software version 9 (Thermo Fisher Scientific, Inc.) for

PLS [23] and PCR. The performance of the multivariate calibration models was evaluated using statistical parameters, including the coefficient of determination (R^2), root mean square error of calibration (RMSEC), and root mean square error of prediction (RMSEP), following previously established methodologies [24,25].

3. RESULTS AND DISCUSSION

Steam distillation of *C. aeruginosa* rhizomes yielded an essential oil with a 2.19% (v/v) concentration. The obtained oil appeared as a clear purple liquid with a characteristic aromatic odor typical of *Curcuma* species and a bitter-pungent taste. The color and odor characteristics are consistent with previously reported descriptions of EOs-CA, which is known to exhibit a bluish-purple hue due to the presence of sesquiterpenoid constituents [26,27]. Based on these typical characteristics, the oil was subsequently analyzed using FTIR spectroscopy to authenticate it.

3.1 FTIR spectra analysis

FTIR spectroscopy was employed in this study due to its capability to provide rapid and direct information on the molecular fingerprint of aromatic essential oils, particularly through the identification of functional groups present within the sample [28]. This method facilitates a more comprehensive and accurate identification of the chemical constituents in EOs [29]. Moreover, the fingerprinting feature of FTIR spectroscopy based on the unique IR spectral profiles of each compound allows for the detection and differentiation of essential oils, as no two distinct compounds exhibit identical infrared spectra. The presence of specific peaks and shoulders in the spectra serves as an indicative marker of unique functional groups, thus enabling differentiation between compounds [30].

FTIR spectra of EOs-CA, EOs-CX, and EOs-CA/EOs-CX are analyzed at 2961, 2926, 2872, 1702, 1653, 1635, 1426, 1374, 1254, 1071, 964, 891, and 749 cm^{-1} , which convey the primary peaks. Meanwhile, EOs-CA/EOs-CX/VCO are analyzed at 2926, 2872, 1702, 1426, and 1071 cm^{-1} , which convey the primary peaks. The vibrational bands at 2961, 1653, 1426, 1071, 964, and 891 cm^{-1} are described by the EOs-CA peak marker. The presence of terpenoid molecules from the sesquiterpene group, including germacrone and curzerenone, in EOs-CA indicates that spectrum characteristics originating from terpenes - CH_3 , - $\text{C}=\text{C}$, and - $\text{C}-\text{H}$ may be present in the stretching and bending vibration. The alkyl groups of methyl (CH_3) and methylene (CH_2) were observed at $1/\lambda$ 2961, 2926, and 2872 cm^{-1} (asymmetric stretching of CH_3 and CH_2). The strong peaks at $1/\lambda$ 1702 cm^{-1} corresponded to unconjugated and conjugated carbonyl ($\text{C}=\text{O}$), respectively, while the peaks at $1/\lambda$ 1653 and 1635 cm^{-1} are due to the absorption of $\text{C}=\text{C}$ in stretching vibration mode [28]. Peaks at $1/\lambda$ 1426 cm^{-1} and 1374 cm^{-1} could be attributed to CH_2 and CH_3 group vibrations in bending mode. Peaks at $1/\lambda$ 1254 and 1071 cm^{-1} are due to the stretching vibration of $\text{C}-\text{O}$. The $\text{C}-\text{OH}$ stretching vibration is represented by the peak at $1/\lambda$ 964 cm^{-1} , whereas the functional groups of - $\text{HC}=\text{CH}$ - (trans) and - $\text{HC}=\text{CH}$ - (cis) out of the plane are the source of the peaks at $1/\lambda$ 891 and 749 cm^{-1} , respectively (Table 3). The functional groups of its fatty acids are responsible for the distinctive bond vibration peaks of VCO: - $\text{C}-\text{H}$ (- CH_2 and - CH_3) stretching at 2954, 2922, and 2853 cm^{-1} ; - $\text{C}-\text{H}$ (- $\text{C}=\text{O}$) stretching at 1741 cm^{-1} ; - $\text{C}-\text{H}$ (- CH_2 and - CH_3) bending at 1467 and 1417 cm^{-1} ; - $\text{C}-\text{O}$ and - $\text{C}-\text{OCH}_2$ stretching and bending at 1228, 1155, and 1111 cm^{-1} ; 721 cm^{-1} for bending of -(CH_2)n- [30,31,32].

Table 3. Identification of functional groups and vibration types from the FTIR spectrum of *C. aeruginosa*

| Wave number (cm^{-1}) | Functional group | Vibration type |
|----------------------------------|---------------------------------|---|
| 2961, 2924 dan 2875 | -C-H | aliphatic -C-H stretching vibration |
| 1743 and 1660 | -C=O | unconjugated and conjugated C=O stretching vibrations |
| 1512 | -C=C | C=C stretching vibration of alkenes |
| 1425 and 1370 | -C-H | bending vibration of CH_2 and CH_3 |
| 1254 dan 1071 | -C-O | C-O stretching vibration |
| 964 | -C-OH | C-OH stretching vibration |
| 891 and 745 | CH=CH- (trans) -CH=CH- (cis) | bending vibration -HC=CH- |

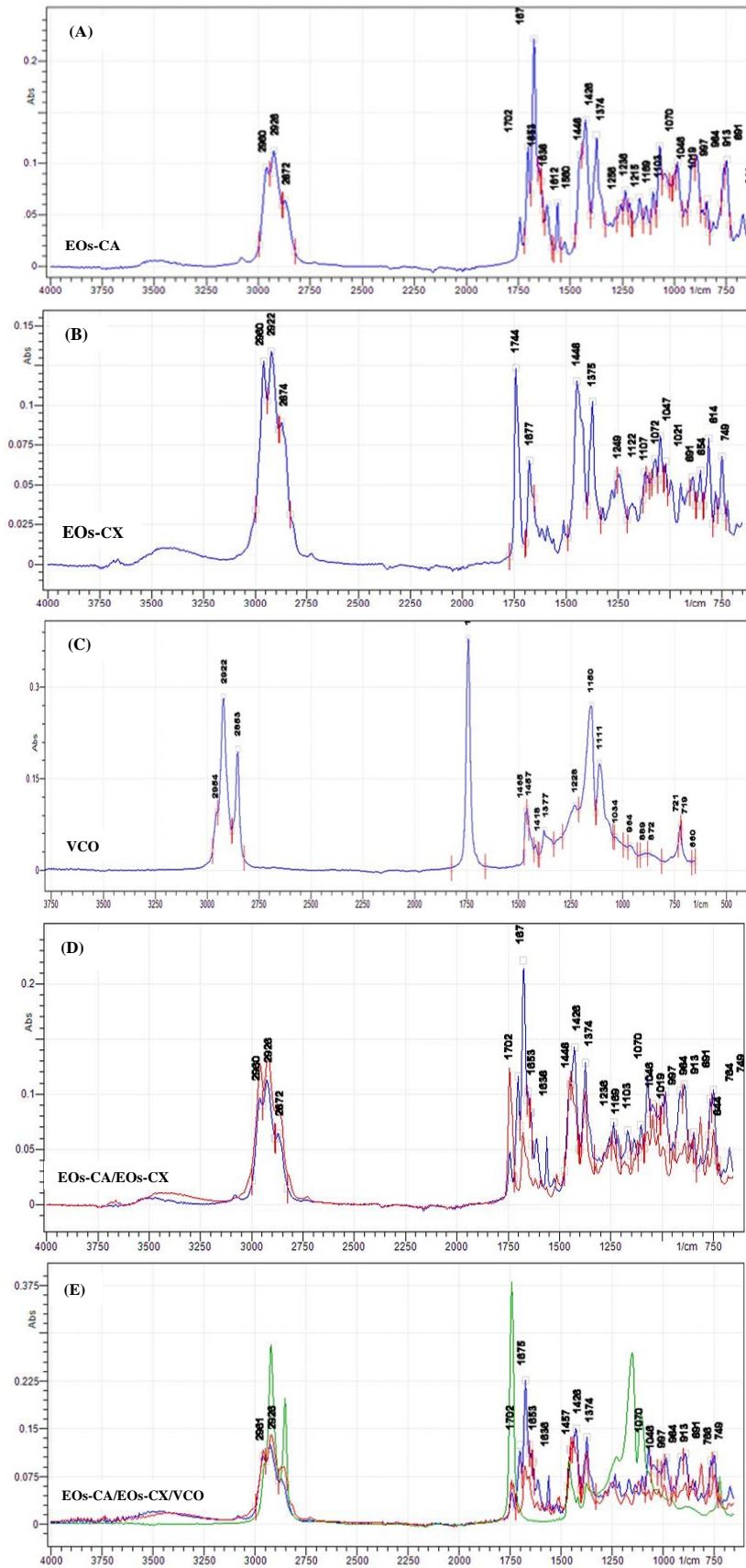


Figure 1. (A) FTIR spectra of EO-CA, (B) EO-CX, (C) VCO, (D). EO-CA adulterated EO-CX (biner), and (E) EO-CA adulterated EO-CX/VCO (ternary)

Figure 1 shows that the binary mixture of EOs-CA and EOs-CX exhibited similar spectral patterns; however, differences in absorbance intensity were observed mainly in the 1702–1685 cm^{-1} region and the fingerprint region 1500–900 cm^{-1} , indicating variations in sesquiterpene composition and therefore requiring chemometric analysis for discrimination. In contrast, the ternary mixture (EOs-CA/EOs-CX/VCO) displayed more evident spectral changes, characterized by increased aliphatic C–H bands (2920–2850 cm^{-1}) and the appearance of a strong ester carbonyl band around 1740 cm^{-1} from triglycerides, along with intensity alterations in the fingerprint region. These results indicate that the binary mixture is detected through relative intensity variations, whereas the ternary mixture is identified by the emergence of new functional groups together with compositional changes.

3.2. Chemometric analysis

Discriminant Analysis (DA), a supervised pattern recognition method [33] was applied to differentiate pure EOs-CA from its binary and ternary mixtures with EOs-CX and VCO. DA classifies samples by calculating the Mahalanobis distance between group centroids and individual data points, allowing identification of groups that are spectrally similar or distinct [34]. The resulting classification models effectively distinguished EOs-CA from both binary (EOs-CX) and ternary (EOs-CX/VCO) adulterated samples, indicating that the spectral features of EOs-CA differ sufficiently from those of the adulterants. The separation between groups was visually confirmed using Coomans plots, which illustrate the residual distances of samples from the independent principal component models of each group [35]. In the binary model, EOs-CA was distinctly separated from EOs-CX (Figure 2), while in the ternary model, EOs-CA showed clear separation from both EOs-CX and VCO (Figure 4).

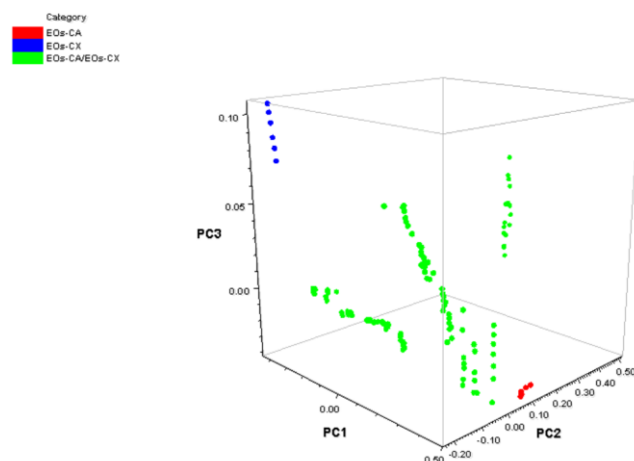


Figure 2. The Coomans plot of FTIR normal spectra in combined frequency ranges of 1770-1100 cm^{-1} for discriminant analysis of EOs-CA, EOs-CX, and EOs-CA/EOs-CX

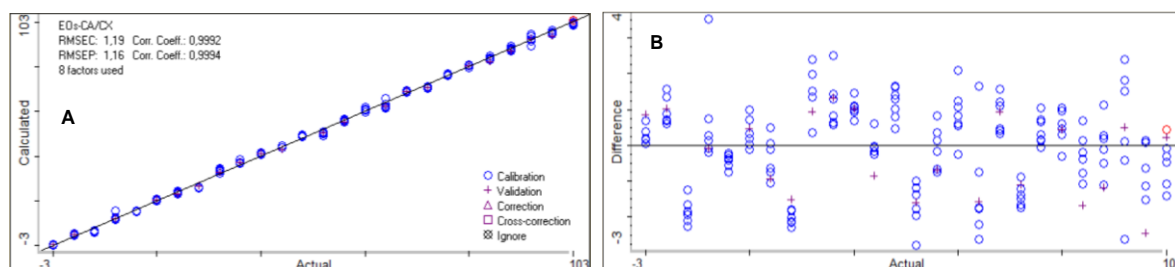


Figure 3. The relationship between EOs-CA's actual values (x-axis) and EOs-CX's predicted values in x-axis utilizing FTIR spectroscopy [A] and residual analysis [B]

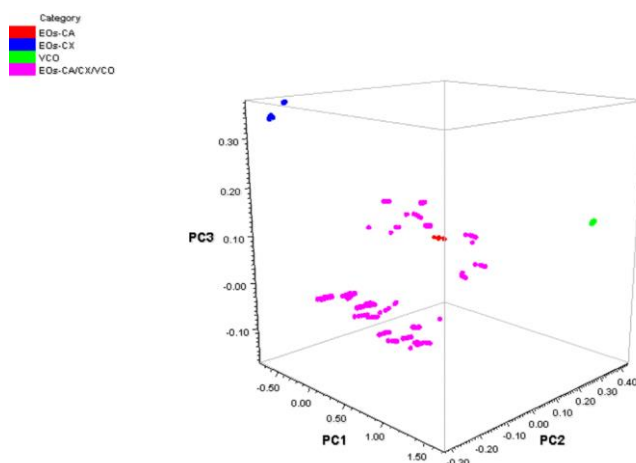


Figure 4. The Coomans plot of FTIR normal spectra in combined frequency ranges of 1770-1100 and 3050-2750 cm^{-1} for discriminant analysis of EO:CA, EO:CX, VCO, and EO:CA/EO:CX-VCO

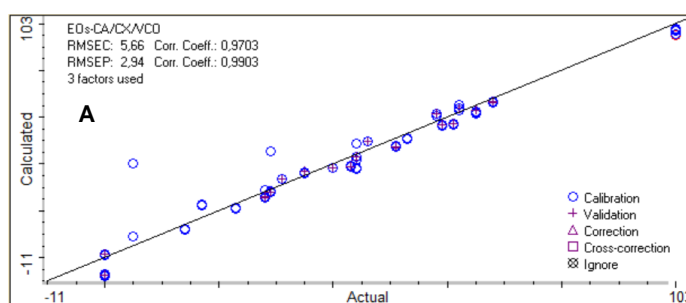


Figure 5. The relationship between EO:CA's actual values (x-axis) and EO:CX/VCO's predicted values in x-axis utilizing FTIR spectroscopy [A] and residual analysis [B]

Meanwhile, Mahalanobis distance, as visualized through the Coomans plot, provides a powerful statistical approach to compare a set of unknown samples against known reference groups based on their multivariate characteristics [36]. In this study, Mahalanobis distance was computed using absorbance values in specific wavenumber regions 1770–1100 cm^{-1} for binary mixtures and 3050–2750 cm^{-1} combined with 1770–1100 cm^{-1} for ternary mixtures. These spectral regions were found to be effective in discriminating EO:CA from adulterants in both binary and ternary systems. This implies a significant potential for detecting adulteration with spectrally similar essential oils (such as EO:CX) or low-value vegetable oils (such as VCO). Multivariate calibration models for both binary and ternary systems were optimized to develop the most accurate and robust prediction tools [37]. FTIR spectral data were subjected to three different preprocessing modes: raw spectra, first derivative, and second derivative. The calibration results, including statistical performance indicators, are summarized in Tables 4 and 5.

The model selection criteria prioritized those with the highest coefficients of determination (R^2) and the lowest error values. For the binary mixtures, Partial Least Squares (PLS) analysis using second derivative spectra in the 1785–728 cm^{-1} range yielded the optimal calibration and validation results. In contrast, for the ternary mixtures, the most accurate predictions were achieved using raw spectra. The calibration and validation R^2 values for the binary mixture model were 0.9992 and 0.9994, respectively (Figure 3), while those for the ternary mixture were 0.9703 and 0.9903 (Figure 5). The Root Mean Square Error of Calibration (RMSEC) for the binary model was 1.19, while the Root Mean Square Error of Prediction (RMSEP) for the ternary model was 5.66 for calibration and 2.94 for validation. These results indicate that the multivariate calibration models developed in this study for both binary and ternary mixtures are highly accurate and reliable. The high R^2 values combined with low RMSEC and RMSEP values reflect strong predictive power and minimal error (38)]. Figures 3 and 5 illustrate the linear correlation between the actual (x-axis) and predicted (y-axis) concentrations

of EOs-CA, demonstrating the effectiveness of FTIR spectroscopy when integrated with chemometric analysis.

Table 4. The performance of PLS and PCR for the quantification of EOs-CA in EOs-CX

| Wavelength | Spectra | PLS | | | | PCR | | | |
|-------------------------|---------------------|----------------|-------------|----------------|-------------|----------------|-------------|----------------|-------------|
| | | Calibration | | Validation | | Calibration | | Validation | |
| | | R ² | RMSEC | R ² | RMSEP | R ² | RMSEC | R ² | RMSEP |
| 3050-728 | Normal | 0.9977 | 2.03 | 0.9984 | 1.75 | 0.9989 | 1.43 | 0.9994 | 1.10 |
| | Derivative 1 | 0.9977 | 2.03 | 0.9984 | 1.75 | 0.9985 | 1.62 | 0.9992 | 1.27 |
| | Derivative 2 | 0.9977 | 2.03 | 0.9984 | 1.75 | 0.9963 | 2.56 | 0.9974 | 2.23 |
| 1785-728 | Normal | 0.9986 | 1.61 | 0.9988 | 1.51 | 0.9987 | 1.51 | 0.9992 | 1.25 |
| | Derivative 1 | 0.9991 | 1.25 | 0.9994 | 1.11 | 0.9988 | 1.44 | 0.9993 | 1.13 |
| | Derivative 2 | 0.9992 | 1.19 | 0.9994 | 1.16 | 0.9985 | 1.65 | 0.9989 | 1.47 |
| 1310-728 | Normal | 0.9981 | 1.85 | 0.9990 | 1.35 | 0.9991 | 1.20 | 0.9993 | 1.17 |
| | Derivative 1 | 0.9988 | 1.49 | 0.9992 | 1.23 | 0.9988 | 1.48 | 0.9993 | 1.15 |
| | Derivative 2 | 0.9990 | 1.36 | 0.9990 | 1.34 | 0.9987 | 1.53 | 0.9992 | 1.24 |
| 1770-1350 | Normal | 0.9983 | 1.76 | 0.9988 | 1.52 | 0.9986 | 1.61 | 0.9988 | 1.49 |
| | Derivative 1 | 0.9978 | 1.98 | 0.9987 | 1.57 | 0.9985 | 1.61 | 0.9989 | 1.46 |
| | Derivative 2 | 0.9983 | 1.73 | 0.9986 | 1.65 | 0.9985 | 1.66 | 0.9987 | 1.71 |
| 960-656 | Normal | 0.9988 | 1.46 | 0.9991 | 1.30 | 0.9987 | 1.52 | 0.9991 | 1.29 |
| | Derivative 1 | 0.9983 | 1.74 | 0.9993 | 1.17 | 0.9986 | 1.59 | 0.9994 | 1.07 |
| | Derivative 2 | 0.9983 | 1.72 | 0.9994 | 1.08 | 0.9982 | 1.78 | 0.9993 | 1.14 |
| 3050-2750 dan 1770-1350 | Normal | 0.9978 | 1.99 | 0.9978 | 2.03 | 0.9984 | 1.67 | 0.9987 | 1.53 |
| | Derivative 1 | 0.9980 | 1.91 | 0.9988 | 1.53 | 0.9986 | 1.61 | 0.9989 | 1.46 |
| | Derivative 2 | 0.9984 | 1.68 | 0.9987 | 1.58 | 0.9986 | 1.59 | 0.9989 | 1.58 |
| 3050-2750 dan 1310-728 | Normal | 0.9981 | 1.83 | 0.9988 | 1.51 | 0.9989 | 1.39 | 0.9992 | 1.20 |
| | Derivative 1 | 0.9987 | 1.52 | 0.9993 | 1.13 | 0.9988 | 1.44 | 0.9993 | 1.12 |
| | Derivative 2 | 0.9991 | 1.27 | 0.9989 | 1.40 | 0.9987 | 1.53 | 0.9991 | 1.30 |

Table 5. The performance of PLS and PCR for the quantification of EOs-CA in EOs-CX/ VCO

| Wavelength | Spectra | PLS | | | | PCR | | | |
|-------------------------|---------------|----------------|-------------|----------------|-------------|----------------|-------------|----------------|-------------|
| | | Calibration | | Validation | | Calibration | | Validation | |
| | | R ² | RMSEC | R ² | RMSEP | R ² | RMSEC | R ² | RMSEP |
| 3050-728 | Normal | 0.9681 | 5.86 | 0.9887 | 3.13 | 0.9732 | 5.38 | 0.9924 | 2.69 |
| | Derivative 1 | 0.9684 | 5.83 | 0.9856 | 3.30 | 0.9722 | 5.47 | 0.9907 | 3.23 |
| | Derivative 2 | 0.9680 | 5.86 | 0.9827 | 3.53 | 0.9736 | 5.33 | 0.9894 | 3.07 |
| 1785-728 | Normal | 0.9703 | 5.66 | 0.9903 | 2.94 | 0.9750 | 5.19 | 0.9927 | 2.57 |
| | Derivative 1 | 0.9675 | 5.91 | 0.9836 | 3.49 | 0.9718 | 5.51 | 0.9888 | 3.39 |
| | Derivative 2 | 0.9664 | 6.01 | 0.9845 | 3.39 | 0.9717 | 5.52 | 0.9894 | 3.39 |
| 1310-728 | Normal | 0.9680 | 5.86 | 0.9814 | 3.85 | 0.9745 | 5.24 | 0.9874 | 3.26 |
| | Derivative 1 | 0.9650 | 6.13 | 0.9748 | 4.66 | 0.9763 | 5.05 | 0.9897 | 2.85 |
| | Derivative 2 | 0.9653 | 6.10 | 0.9711 | 4.95 | 0.9695 | 5.73 | 0.9906 | 3.08 |
| 1770-1350 | Normal | 0.9679 | 5.78 | 0.9907 | 2.95 | 0.9757 | 5.12 | 0.9925 | 2.67 |
| | Derivative 1 | 0.9633 | 6.27 | 0.9764 | 4.05 | 0.9754 | 5.15 | 0.9913 | 3.00 |
| | Derivative 2 | 0.9623 | 6.23 | 0.9789 | 3.86 | 0.9747 | 5.22 | 0.9847 | 3.65 |
| 960-656 | Normal | 0.9464 | 6.16 | 0.9810 | 3.99 | 0.9764 | 5.05 | 0.9928 | 2.62 |
| | Derivative 1 | 0.9670 | 5.95 | 0.9853 | 3.82 | 0.9702 | 5.67 | 0.9910 | 3.41 |
| | Derivative 2 | 0.9694 | 5.73 | 0.9862 | 4.04 | 0.9699 | 5.69 | 0.9860 | 3.63 |
| 3050-2750 dan 1770-1350 | Normal | 0.9645 | 6.17 | 0.9855 | 3.65 | 0.9759 | 5.10 | 0.9939 | 2.61 |
| | Derivative 1 | 0.9657 | 6.07 | 0.9814 | 3.65 | 0.9755 | 5.14 | 0.9908 | 3.07 |
| | Derivative 2 | 0.9625 | 6.34 | 0.9794 | 3.82 | 0.9752 | 5.17 | 0.9861 | 3.60 |
| 3050-2750 dan 1310-715 | Normal | 0.9666 | 5.99 | 0.9845 | 3.50 | 0.9744 | 5.25 | 0.9894 | 2.81 |
| | Derivative 1 | 0.9669 | 5.97 | 0.9805 | 4.19 | 0.9765 | 5.04 | 0.9914 | 2.95 |
| | Derivative 2 | 0.9661 | 6.03 | 0.9744 | 4.70 | 0.9737 | 5.33 | 0.9822 | 3.82 |

As shown in Table 5, compared to the binary mixture, the ternary mixture model exhibited slightly lower R^2 values and higher errors due to increased complexity caused by the presence of two adulterants. However, the PLS model still outperformed PCR across all wavenumber regions. An R^2 value in chemometric models does not necessarily need to reach 0.99, particularly for complex herbal matrices. In natural product extracts, overlapping signals, biological variability, and reference method uncertainty limit the achievable correlation. Therefore, the obtained calibration R^2 of approximately 0.97 already indicates excellent predictive performance and is acceptable for FTIR chemometric analysis.

Moreover, the application of derivative spectral preprocessing effectively resolved issues associated with overlapping absorption bands, although it may slightly reduce sensitivity [39]. The selection of the higher wavenumber range contributed significantly to obtaining higher R^2 values across both mixture types. Ultimately, FTIR spectroscopy combined with multivariate calibration techniques such as PLS has proven to be a rapid and robust approach for the quantitative authentication of the essential oils [40,41].

4. CONCLUSION

Fourier Transform Infrared (FTIR) spectroscopy, in combination with Discriminant Analysis (DA), Partial Least Squares (PLS), and Principal Component Regression (PCR), has proven to be an effective analytical approach for the authentication of *Curcuma aeruginosa* essential oil (EOs-CA) in both binary and ternary mixtures. The second derivative of the FTIR-ATR spectra, specifically in the combined wavenumber region of 1785–728 cm^{-1} , was identified as the most suitable spectral range for the quantitative analysis of EOs-CA in binary mixtures with *C. xanthorrhiza* (EOs-CX), as well as in ternary mixtures containing EOs-CX and Virgin Coconut Oil (VCO). The combination of FTIR spectroscopy with DA and multivariate calibration methods such as PLS enables accurate discrimination between pure and adulterated EOs-CA, offering a rapid, non-destructive, and reliable technique for quality control in essential oil authentication.

Funding: This research was funded by the Ministry of Higher Education, Science, and Technology of the Republic of Indonesia, grant number: 03157/BPPT/BPI.06/9/2024

Acknowledgments: The authors would like to thank the Indonesian Education Scholarship (BPI), the Center for Higher Education Funding and Assessment (PPAPT), the Ministry of Higher Education, Science, and Technology of the Republic of Indonesia, and the Indonesian Endowment Fund for Education (LPDP) for supporting this research.

Conflicts of interest: The authors declare no conflict of interest.

References

1. von Rintelen K, Arida E, Häuser C. A review of biodiversity-related issues and challenges in megadiverse Indonesia and other Southeast Asian countries. *Res Ideas Outcomes*. 2017;3:1–16.
2. Sukardiyono, Rosana D. Megabiodiversity Utilization through Integrated Learning Model of Natural Sciences with Development of Innertdepend Strategies in Indonesian Border Areas. *J Phys Conf Ser*. 2019;1233(1):1–11.
3. Paramita S, Moerad EB, Ismail S, Marliana E. Antiasthmatic effect of *Curcuma aeruginosa* extract on isolated organ of the trachea. *F1000Research*. 2018;7(1779):1–6.
4. Sari AP. Phytochemistry and biological activities of *Curcuma aeruginosa* (Roxb.). *Indones J Chem*. 2022;22(2):576–98.
5. Nugraheni B, Rohman A, Susidarti RA, Purwanto P. Tropical Journal of Natural Product Research Influence of Geographical Origin on Essential Oil Contents in *Curcuma aeruginosa* Roxb. Rhizomes in Central Java, Indonesia. *Trop J Nat Prod Res [Internet]*. 2024;8(12):9596–602. Available from: <https://www.tjnpr.org>
6. Kamazeri TSAT, Samah OA, Taher M, Susanti D, Qaralleh H. Antimicrobial activity and essential oils of *Curcuma aeruginosa*, *Curcuma mangga*, and *Zingiber cassumunar* from Malaysia. *Asian Pac J Trop Med*. 2012;5(3):202–9.
7. Angel G. Phenolic content and antioxidant activity in five underutilized starchy *Curcuma* species. *Int J Pharmacogn Phytochem Res*. 2012;4(2):69–73.

8. Theanphong, Mingvanish W, Kirdmanee C. Chemical constituents and biological activities of essential oil from *Curcuma aeruginosa* Roxb. Rhizome. Sci Technol BHST. 2015;13(1):6–16.
9. Poudel DK, Ojha PK, Rokaya A, Satyal R, Satyal P, Setzer WN. Analysis of volatile constituents in *Curcuma* Species, viz. *C. aeruginosa*, *C. zedoaria*, and *C. longa*, from Nepal. Plants. 2022;11(15):2–12.
10. George M, Britto SJ. Phytochemical and antioxidant studies on the essential oil of the rhizome of *Curcuma aeruginosa* Roxb. Int Res J Pharm. 2015;6(8):573–9.
11. Akarchariya N, Sirilun S, Julsrigival J, Chansakaowa S. Chemical profiling and antimicrobial activity of essential oil from *Curcuma aeruginosa* Roxb., *Curcuma glans* K. Larsen & J. Mood and *Curcuma cf. xanthorrhiza* Roxb. collected in Thailand. Asian Pac J Trop Biomed. 2017;7(10):881–5.
12. Aziz JA, Saidi NB, Ridzuan R, Mohammed AKS, Abdul Aziz M, Abdul Kadir M. Chemical profiling of *Curcuma aeruginosa* Roxb. essential oil and their antimicrobial activity against pathogenic microbes. J Essent Oil-Bearing Plants. 2021;24(5):1059–71.
13. Moreira da Silva T, Pinheiro CD, Puccinelli Orlandi P, Pinheiro CC, Soares Pontes G. Zerumbone from *Zingiber zerumbet* (L.) smith: A potential prophylactic and therapeutic agent against the cariogenic bacterium *Streptococcus mutans*. BMC Complement Altern Med. 2018;18(1).
14. Widjajanti H, Handayani CV, Nurnawati E. Antibacterial activity of endophytic fungi from sembukan (*paederia foetida* l.) leaves. Sci Technol Indones. 2021;6(3):189–95.
15. Gusti N, Oktarina D, Elvia R, Nursa'adah E, Wardhana RW, Sundaryono A, et al. Facile detection of oil adulteration using uv-visible spectroscopy coupled with chemometric analysis. Sci Technol Indones. 2021;6(1):14–8.
16. Syafri S, Jaswir I, Yusof F, Rohman A, Hamidi D. The use of GC-MS and FTIR spectroscopy coupled with multivariate analysis for the detection of Red Ginger oil adulteration. Rasayan J Chem. 2022 Oct 1;15(4):2231–6.
17. Anggriani F, Rohman A, Martien R. The Employment of ATR-FTIR Spectroscopy and Chemometrics for Authentication of Bawal (*Colossoma macromopum*) Fish Oil from Palm Oil [Internet]. Vol. 2024, J.Food Pharm.Sci. Available from: www.journal.ugm.ac.id/v3/JFPS
18. Rohman A, Ariani R. Authentication of nigella sativa seed oil in binary and ternary mixtures with corn oil and soybean oil using FTIR spectroscopy coupled with partial least square. Sci World J. 2013;2013:1–6.
19. Khudzaifi M, Retno SS, Rohman A. The employment of FTIR spectroscopy and chemometrics for authentication of essential oil of *Curcuma mangga* from candle nut oil. Food Res. 2020;4(2):515–21.
20. Syafri S, Sabilla AN, Rahma Dewiana S, Ulwafi D, Syofyan S, Hamidi D, et al. Rapid Identification of Turmeric (*Curcuma longa*) Essential Oil Authenticity using FTIR Spectroscopy Coupled with Chemometrics. Malaysian J Chem. 2025;27(4):172–81.
21. Truzzi E, Marchetti L, Bertelli D, Benvenuti S. Attenuated total reflectance–Fourier transform infrared (ATR–FTIR) spectroscopy coupled with chemometric analysis for detection and quantification of adulteration in lavender and citronella essential oils. Phytochem Anal. 2021;32(6):907–20.
22. Taylan O, Cebi N, Sagdic O. Rapid screening of mentha spicata essential oil and l-menthol in mentha piperita essential oil by atr-ftir spectroscopy coupled with multivariate analyses. Foods. 2021 Feb 1;10(2):2–14.
23. Rizky Elvira A, Rosiana Putri A, Ahmad Muchlashi L. Detection of Garlic Powder Adulteration Using FTIR Spectroscopy and Chemometrics: A Case Study in an Indonesia Marketplace [Internet]. Vol. 2024, J.Food Pharm.Sci. Available from: www.journal.ugm.ac.id/v3/JFPS
24. Hirri A, Bassbasi M, Platikanov S, Tauler R, Oussama A. FTIR spectroscopy and PLS-DA classification and prediction of four commercial grade Virgin olive oils from Morocco. Food Anal Methods. 2016 Apr 1;9(4):974–81.
25. Purwakusumah ED, Rafi M, Syafitri UD, Nurcholis W, Agung M, Adzkiya Z. Identification and Authentication of Jahe Merah Using Combination of FTIR Spectroscopy and Chemometrics. AGRITECH. 2014;34(1):82–7.
26. Waras N, Nurul K, Muhamad S, Maria B, Ardyani IDAAC. Phytochemical screening, antioxidant and cytotoxic activities in extracts of different rhizome parts from *Curcuma aeruginosa* Roxb. Int J Res Ayurveda Pharm. 2015;6(5):634–7.
27. Nugraheni B, Rohman A, Susidarti RA, Purwanto. Review of essential oils of *Curcuma aeruginosa*: chemical composition and pharmacological activities. Food Res [Internet]. 2026 Jan 4;10(1):1. Available from: https://www.myfoodresearch.com/uploads/8/4/8/5/84855864/_1_fr-2023-253_nugraheni.pdf
28. Bunaciu AA, Aboul-Enein HY, Fleschin S. Recent applications of fourier transform infrared spectrophotometry in herbal medicine analysis. Appl Spectrosc Rev. 2011;46(4):251–60.
29. Agatonovic-Kustrin S, Ristivojevic P, Gegechkori V, Litvinova TM, Morton DW. Essential oil quality and

- purity evaluation via ft-ir spectroscopy and pattern recognition techniques. Appl Sci. 2020;10(20):1–12.
30. Bendini A, Cerretani L, Di Virgilio F, Belloni P, Bonoli-Carbognin M, Lercker G. Preliminary evaluation of the application of the FTIR spectroscopy to control the geographic origin and quality of virgin olive oils. J Food Qual. 2007;30:424–37.
 31. Nugraheni B, Rohman A, Susidarti RA, Purwanto P. Fourier transform infrared spectroscopy combined with chemometrics for quality control of *Curcuma aeruginosa* rhizomes: An essential oil analysis. J Adv Pharm Technol Res. 2024;15(4):248–57.
 32. De Luca M, Ioele G, Grande F, Occhiuzzi MA, Chieffallo M, Garofalo A. Multivariate curve resolution methodology applied to the ATR-FTIR data for adulteration assessment of Virgin coconut oil. Molecules [Internet]. 2023;28(12):1–13. Available from: <https://www.preprints.org/manuscript/202305.0634/v1>
 33. Septyanti C, Batubara I, Rafi M. HPLC fingerprint analysis combined with chemometrics for authentication of kaempferia galanga from related species. Indones J Chem. 2016;16(3):308–14.
 34. Rohman A, Man YBC. The chemometrics approach applied to FTIR spectral data for the analysis of rice bran oil in extra virgin olive oil. Chemom Intell Lab Syst. 2012 Jan 15;110(1):129–34.
 35. Talib RA, Rashid NM, Rahman RA, Mohamad N, Sukor R, Mohamad Mazlan M. Coomans plot classification of lard in the ink blends and ink extracts from printed packaging films using lard Fourier transform infrared spectral profile and multivariate analysis. Food Res. 2024 Jul 15;8(4):108–16.
 36. Ballabio D, Todeschini R. Multivariate classification for qualitative analysis. In: Da-Wen Sun, editor. Infrared spectroscopy for food quality analysis and control. Elsevier Inc; 2009. p. 97–9.
 37. Fatmarahmi DC, Susidarti RA, Swasono RT, Rohman A. Application of FTIR-ATR spectroscopy in combination with multivariate analysis to analyze synthetic drugs adulterant in ternary mixtures of herbal medicine products. Indones J Pharm. 2022;33(1):63–71.
 38. Salamah N, Nining Handaningrum K, Guntarti A, Helal Uddin A, Ahda M. Authentication of Lemongrass (*Cymbopogon citratus*) and Citronella (*Cimbopogon nardus*) essential oils in fragrance products using FTIR spectroscopy combined with chemometrics. Malaysian J Chem. 2025;27(4):198–206.
 39. Rohman A. Spektroskopi Inframerah dan Kemometrika untuk Analisis Farmasi. 1st ed. Yogyakarta: Pustaka Pelajar; 2014. 199–225 p.
 40. Siregar C, Martono S, Rohman A. Application of Fourier transform infrared (FTIR) spectroscopy coupled with multivariate calibration for quantitative analysis of curcuminoid in tablet dosage form. J Appl Pharm Sci. 2018 Aug 1;8(8):151–6.
 41. Andina L, Saputri R, Novyra Putri A, Lukitaningsih E, Rohman A. Analysis of Adulterated Pangasius Hypophthalmus Oil by ATR-FTIR Spectroscopy and Chemometric [Internet]. Vol. 2019, J.Food Pharm.Sci. Available from: www.journal.ugm.ac.id/v3/JFPS



© 2026 by the authors. Submitted for possible open access publication under the terms and conditions of the Creative Commons Attribution (CC BY) license (<http://creativecommons.org/licenses/by/4.0/>).